Applied Physics Letters ARTICLE scitation.org/journal/apl

Compressed liquid marble ruptures at edge

Cite as: Appl. Phys. Lett. **114**, 243701 (2019); doi: 10.1063/1.5108999
Submitted: 5 May 2019 · Accepted: 31 May 2019 ·
Published Online: 19 June 2019

Zhou Liu,[1,2,a)] Yage Zhang,[2] Tiyun Yang,[1] Zhi Wang,[1] and Ho Cheung Shum[2,a)]

AFFILIATIONS

[1]College of Chemistry and Environmental Engineering, Shenzhen University, Shenzhen, Guangdong 518000, China
[2]Department of Mechanical Engineering, The University of Hong Kong, Pokfulam Road, Hong Kong, China

[a)]**Authors to whom correspondence should be addressed:** zhouliu@szu.edu.cn and ashum@hku.hk

ABSTRACT

An improved understanding of the rupture dynamics for liquid marbles is essential for their application in sensors, miniaturized reactions, biomedical scaffolds, the synthesis of functional materials, and others. This work suggests that a compressed liquid marble always ruptures at the edge of the contact area between the marble and a substrate. The rupture dynamics of a compressed marble is visualized with a particle-level resolution using a marble coated with monodispersed microparticles. High-speed photography indicates that the particle density decreases significantly from the center to the edge, and the sparse particle layer at the edge initiates rupturing. Such a particle density distribution is well depicted with our proposed model, which predicts the theoretical values that agree well with the experimental results. This study generalizes the understanding for the rupture dynamics of particle-stabilized droplets and is beneficial to any applications that involve the rupture or coalescence of liquid marbles as well as Pickering emulsions.

Particles can be irreversibly adsorbed onto liquid interfaces to serve as effective additives for droplet stability.[1] This strategy is ubiquitous with examples that include rain droplets coated by sand grains in nature,[2] crude oil droplets stabilized by clay particles in industrial processes,[3] and fat globule-stabilized ice cream foams in foods.[4] Deliberately coating a droplet with nonwetting particles forms a "liquid marble" which has a nearly 180° contact angle with the substrate.[5,6] As the contact line between the liquid and the substrate is eliminated due to the coating particles, liquid marbles represent a competitive alternative to superhydrophobic surfaces, which normally involve sophisticated surface modifications.[7,8] These are advantageous when handling microliter liquids without loss or contamination and have been applied in numerous applications, including miniaturized reactions,[9–11] biomedical scaffolds,[12,13] sensors,[14,15] and the synthesis of functional materials.[16,17] However, these particle-armored drops can only sustain mechanical pressures that range from tens to hundreds of Pascal and can easily rupture under mechanical shock or compression.[18,19] Unlike Pickering emulsions, which are droplets that are stabilized by particles dispersed in another immiscible phase, the rupture process of liquid marbles does not involve particle migration from the outer phase to the droplet surface.[1] Therefore, their different rupture mechanism needs further clarification.

At small deformations, the spring constant or the effective surface tension of a liquid marble can be analyzed using its stress–strain relationship.[20–26] For instance, a squeezed liquid marble exhibits elastic properties with a reversible deformation that is as high as 30%.[24] Such elastic properties can be interpreted using a model based on the growth of the marble surface area considering the conservation of the marble volume.[25,26] The stress–strain relationship of the squeezed liquid marble can be further quantified using an expression that considers its Bond number.[23] In addition, the effective surface tension of a liquid marble can be achieved from its deformed state and has been found to be different from that of a pure liquid core.[26] Recently, using controllable nanoparticle monolayers, the effective surface tension of a marble was found to only reflect its macroscopic properties rather than interparticle forces.[20,21,27,28] Under a large mechanical pressure or shock, the deformation of liquid marbles is irreversible and there exists a critical pressure that causes the marble to rupture. Extensive studies have elucidated various contributing factors that affect the stability of liquid marbles, including the properties of the coating particles,[18,29] the interior liquid,[30] the contact angle,[31] and the volume of marble.[22]

The prevailing explanation for rupture in the two methods is relatively simple. The surface area of a marble increases as it is flattened under compression due to squeezing or impacting. At a critical compression, the coating particles become sufficiently sparse, and so the interior liquid inevitably comes into contact with the substrate, resulting in the marble rupture.[7] However, this interpretation does not illustrate the locational details or dynamics of the coating particles during rupture. Thus, the initiation of the liquid marble rupture remains

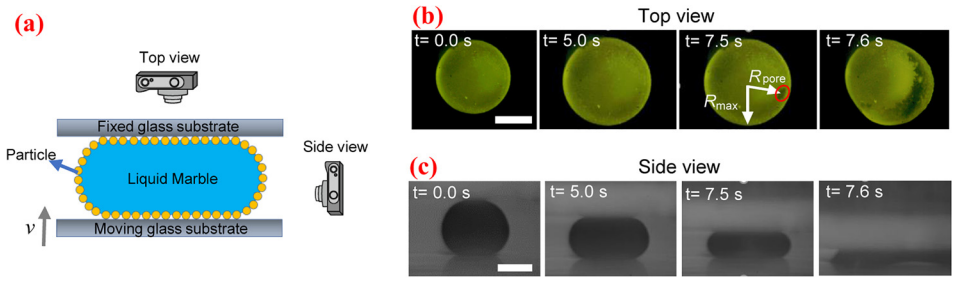

FIG. 1. (a) Schematic of the experimental setup. Images from (b) top view and (c) side view demonstrate the liquid marble under gradual compression until rupture. The red circle indicates the pore where rupture initiates. The compressed marble is water ($R_0 = 0.9$ mm) stabilized with PTFE ($a = 35\ \mu$m) particles. The scale bars are 1 mm.

unknown. These missing pieces of information could be important for better understanding the stability of particle-armored droplets or bubbles.

In this work, we focus on the rupture dynamics of a compressed liquid marble and find that the rupture always occurs at the edge of the contact area between the marble and a substrate. We visualize the edge-rupture phenomenon using liquid marbles coated with monodispersed microparticles where the particle density significantly decreases from the center to the edge. When the edge is barely coated with particles, the interior liquid wets the substrate and triggers a rupture. We further attribute such a particle distribution to the friction between the particles and the substrate, which inhibits the movement of particles, and propose a model to predict the particle density distribution at the contact surface. Our theoretical predictions are consistent with the experimental results, which provide insight into the rupture dynamics of liquid marbles and can be potentially extended to better understand the robustness of other systems involving particulate stabilizers.

To create the liquid marbles, we deposit 3 μL (unless otherwise noted) of de-ionized water droplets on a substrate covered with the stabilizing particles. The particles include two sizes of polytetrafluoroethylene (PTFE) (average particle size $a = 1\ \mu$m and 35 μm; Sigma-Aldrich, USA), uniform silica particles (particle size $a = 6\ \mu$m; Tospearl 2000B*, Momentive Performance Material Inc., Japan), fumed silica particles (primary particle size $a = 7$ nm; Aerosil R812, Evonik, Germany), or polystyrene particles (particle size $a = 50$, 75, 100, 150 μm; NanoMicro Tech. Inc., China). After rolling off the droplets on the particle layers several times, the stabilizing particles are irreversibly adsorbed on the droplet surface to form the liquid marbles. We carefully transport the formed liquid marble onto the bottom glass substrate of a custom-built compression platform, as shown schematically in Fig. 1(a). On top of the marble, a second glass substrate is controlled using a step motor that slowly moves downwards at a speed of $v = 50\ \mu$m/s. As the top substrate approaches, the liquid marble is compressed and becomes flattened until rupture. At the same time, the morphology of the marble and the particle distributions are captured using high-speed cameras (Phantom v9.1) from both the top and side views.

The liquid marbles stabilized with different particles are compressed using the custom-built device shown schematically in Fig. 1(a). Before each compression, the liquid marble remains largely spherical, as shown in Fig. 1(c). When the liquid marble is compressed, it becomes flattened, and the contact area between the marble surface and the substrate gradually extends [t = 0–7.5 s, Fig. 1(b)]. The compressed liquid marble develops a disk shape relative to the substrate, which is nonwetting, as shown from the side view in Fig. 1(c). At a critical extension of the liquid marble, the liquid core rapidly wets the substrate at one of the pores [red circle, t = 7.5 s, Fig. 1(b)] and causes the marble to rupture [t = 7.6 s, Fig. 1(b)].[6,19] The Reynolds number of the liquid marble is $\mathrm{Re} \sim \rho V R_0/\eta \gg 1$,[32] where ρ, V, R_0, and η are the density, characteristic velocity, initial droplet radius, and viscosity, respectively. This suggests that the hydrodynamics are driven by inertial force. Therefore, we estimate the inertial characteristic time of the liquid marble to be $t_\gamma = \sqrt{\rho R_0^3/\gamma}$, where γ is the effective surface tension.[33] Considering that t_γ is much shorter than the time of the compression process, the marble compression can be treated as quasistatic.

Interestingly, we find that the rupture always initiates at a location close to the edge of the contact area. To quantitatively demonstrate this, we characterize the location where the rupture initiates and illustrate it with a polar plot (Fig. 2). For each location, the data of the normalized radius are represented as $R^* = R_{pore}/R_{max}$, where R_{pore} is the distance from the marble center to the pore where the rupture initiates and R_{max} denotes the maximum radius of the flatted marble, as shown in Fig. 1(b). The reported angle of the data refers to the original angle of the pore in the contact area. We systematically characterize the regions where rupture occurs by testing water marbles with different radii R_0 (circle: 0.9 mm; triangle: 1.3 mm; and square: 1.6 mm) and stabilizing particle types (red: PTFE particles with $a = 35\ \mu$m; blue: PTFE particles with $a = 1\ \mu$m; green: silica particles with $a = 6\ \mu$m;

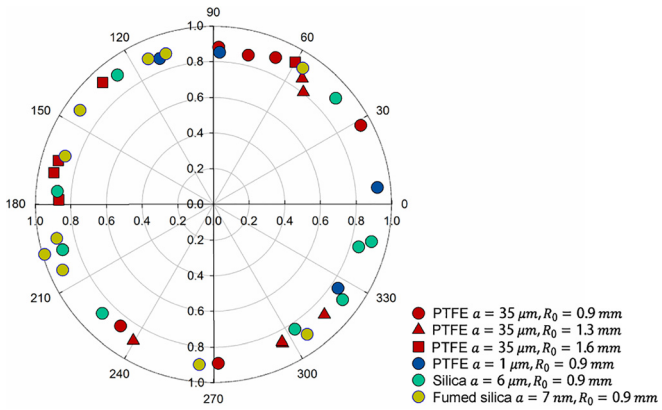

FIG. 2. Polar plot demonstrating the rupture locations of the compressed marbles with different initial sizes R_0 (circle: 0.9 mm; triangle: 1.3 mm; and square: 1.6 mm) and coated using different particles (red dots: PTFE particles with $a = 35\ \mu$m; blue dots: PTFE particles with $a = 1\ \mu$m; green dots: silica particles with $a = 6\ \mu$m; and yellow dots: fumed silica particles with $a = 7$ nm). The data for the radius are normalized by R_{pore}/R_{max}. The reported angles refer to the original angles of the pores where the rupture initiates.

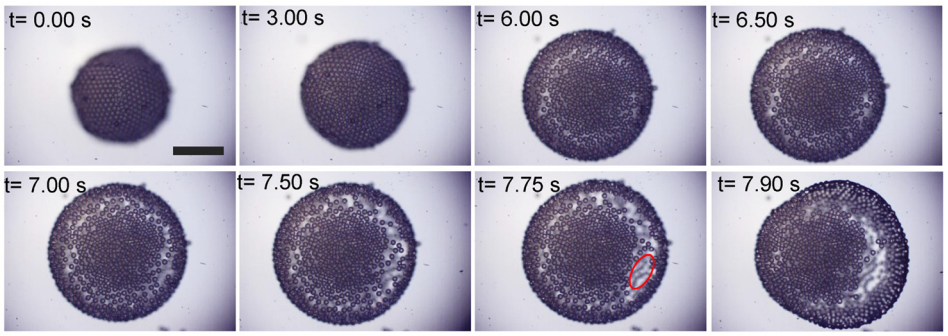

FIG. 3. Top view of micrographs demonstrating the rupture dynamics of the gradually compressed marbles. The red circle indicates the pore where the rupture initiates. The compressed marble has a radius R_0 of 0.9 mm and is stabilized with 100 μm polystyrene particles. The scale bar is 1 mm.

and yellow: fumed silica particles with $a = 7$ nm). All the tested results verify our previous observations that the rupture of a compressed liquid marble indeed initiates at locations close to the edge with R^* ranging from 0.8 to 1, as shown in Fig. 2.

The prevailing reasoning reveals that the rupture of the compressed marble is a simple process. The marble becomes flattened due to compression, and its surface area increases significantly. This reduces the density of coating particles and induces a rupture when the particle layer can no longer sustain the compression. However, this interpretation does not illustrate the dynamic details of the rupture and cannot address the underlying question of how the rupture initiates at the edge. To understand this, the relationship between the local particle distribution and the global rupture dynamics needs further clarification. Therefore, we use microscale polystyrene particles to stabilize the liquid marble. Such polystyrene particles have diameters of 100 μm with a polydispersity of 3%, enabling the visualization of the rupture dynamics at the particle-level resolution under a microscope. Interestingly, this direct observation suggests that the particle density decreases from the center to the edge during the compression, as shown in Fig. 3 (from t = 0 to 7.75 s). At a critical extension of the liquid marble, the liquid core rapidly wets the substrate at the edge covered with the sparse particles and a rupture occurs (t = 7.75 and 7.9 s, Fig. 3).

To further quantify our observations, we analyze the micrographs of the compressed marble and characterize the particle density along the radius x of the contact area using the normalized particle density of σ_x/σ_0, where σ_x is the particle density at a radius x and σ_0 is the initial particle density [Fig. 4(a)]. We count the number of particles N on an annulus with inner and outer radii of $x - dx/2$ and $x + dx/2$, respectively [Fig. 4(a)]. This is then quantified by σ_x as

$$\sigma_x = \frac{N}{\pi x dx}. \tag{1}$$

We systematically compress the liquid marbles stabilized with 50 μm (red triangles), 75 μm (green circle), and 100 μm (blue squares) polystyrene particles and characterize their corresponding particle distributions across the contact area. The results indicate that the normalized particle density σ_x/σ_0 indeed decreases as the normalized radius x/R_0 increases, as shown in Fig. 4(b). These results also confirm that the gradually compressed liquid marble has a decreased particle density at the contact area from the center to the edge. Eventually, the marble rupture initiates at the edge R of the contact area with the loosely packed particles.

One essential question that remains unclear is how the particles distribute loosely at the edges. We propose a model based on the extension of the marbles to elucidate this. Upon compression, the liquid marble adopts a disklike shape that consists of three surfaces. Two surfaces S_{cont} come into contact with the top substrate and bottom substrate, and the third surface S_{free} is between the first two and encircles the disk-shaped marble, as shown schematically in Fig. 4(a). At the center, the particle density should be equal to the initial particle density σ_0. At the same time, the particles at S_{free} are evenly distributed with the same density as those at the edge R of the contact surface σ_R. Due to the friction between the particles and the substrates, the particle movement is inhibited once they are pinned at the contact areas of the substrates. As the particles are irreversibly adsorbed onto the droplet, they should be conserved at any state of compression, which gives

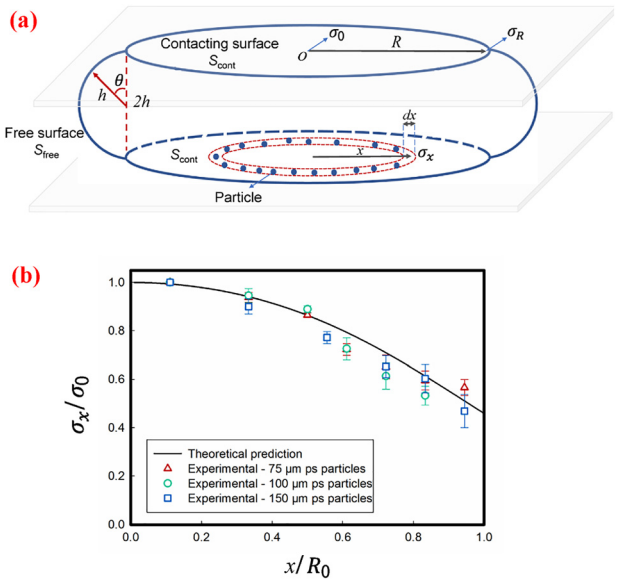

FIG. 4. (a) Schematic of the compressed liquid marble. (b) Normalized particle density σ_x/σ_0 distribution along the normalized radius x/R_0 of the contact area. The tested liquid water marbles have a radius of $R_0 = 0.9$ mm and are stabilized using monodispersed polystyrene particles with different sized a: 75 μm (triangle dots), 100 μm (circle dots), and 150 μm (square dots).

$$S\sigma_R + 2\int_0^R 2\sigma_x \pi x dx = 4\pi R_0^2 \sigma_0, \quad (2)$$

where R_0 is the initial radius of the liquid marble and S is the surface area of the free surface. The first and second terms on the left-hand side of Eq. (2) represent the number of particles on the free surface S and the contact areas, respectively. The right-hand side of Eq. (2) refers to the particles on the marble surface at the initial state before compression. Taking the derivative of Eq. (2) with respect to R gives

$$(4\pi R + S')\sigma_R + S\sigma_R' = 0. \quad (3)$$

Solving Eq. (3) and satisfying the boundary condition of $\sigma_R = \sigma_0$ at $R = 0$, we arrive at the expression for σ_R as

$$\sigma_R = \sigma_0 e^{\int_0^R \frac{4\pi R + S'}{S} dx}. \quad (4)$$

To solve σ_R, we need to know the free surface area S as a function of R. Considering that the liquid marble has a nearly 180° contact angle with the substrate, we can estimate S as

$$S = \int_0^\pi 2\pi(R + h\sin\theta)hd\theta, \quad (5)$$

where $2h$ indicates the height of the squeezed marble. Moreover, we can build the relation of h and R considering the conservation of the marble volume as

$$\frac{4\pi}{3}R_0^3 = 2\pi R^2 h + \int_0^\pi \pi(R + h\sin\theta)^2 h\sin\theta d\theta. \quad (6)$$

The left-hand side of Eq. (6) represents the initial volume of the marble, while the right-hand side includes the volume of the column with a radius of R and height of h, as well as the volume that encircles it. Combining Eqs. (4)–(6) and inputting $R_0 = 0.9$ mm, we numerically solve for the distribution of the dimensionless particle density σ_R/σ_0. As R gradually increases during compression, it is reasonable to assume that the particles that are already pinned at S_{cont} do not move due to the friction between the surface and the substrate. Thus, the particle density σ_R also represents the particle distribution σ_x along the radius x of the contact area. We plot the theoretical prediction of σ_x as the blue line in Fig. 4(b), which shows good agreement with the experimental data. This verifies our model as a predictor of the particle distribution at the contact area of the compressed marble.

In conclusion, we have found and detailed the mechanism that the compressed liquid marble always ruptures at the edge. Using liquid marbles stabilized with monodispersed microparticles, we visualize the particle distribution at the contact area between the compressed marble and the substrate. Further quantitative measurements suggest that the particle density significantly decreases from the center to the edge when the marble is gradually compressed. Consequently, the marble ruptures at the edge where the surface is more loosely packed with particles. In addition, we propose an analytical model to explain the distribution of the particles, which agrees well with the experimental results. Our work extends the understanding of the rupture dynamics for liquid marbles and could inspire future studies on coalescence involving particle-stabilized droplets.

This work was supported by the National Natural Science Foundation of China (No. 21706161), Natural Science Foundation of Guangdong (No. 2017A030310444), Shenzhen Overseas High-level Talents Key Foundation for Innovation and Entrepreneurship and the General Research Fund (Nos. 17304514 and 17329516), and the Research Grants Council of Hong Kong for their financial support.

REFERENCES

[1]B. P. Binks and T. S. Horozov, *Colloidal Particles at Liquid Interfaces* (Cambridge University Press, 2006).
[2]C. V. Boys, *Soap Bubbles, Their Colours and the Forces Which Mold Them* (Courier Corporation, 1959).
[3]D. E. Tambe and M. M. Sharma, Adv. Colloid Interface Sci. **52**, 1 (1994).
[4]A. W. Adamson and A. P. Gast, *Physical Chemistry of Surfaces* (Interscience, New York, 1967).
[5]P. Aussillous and D. Quéré, Nature **411**, 924 (2001).
[6]P. Aussillous and D. Quéré, Proc. R. Soc. A: Math. Phys. Eng. Sci. **462**, 973 (2006).
[7]G. McHale and M. I. Newton, Soft Matter **7**, 5473 (2011).
[8]E. Bormashenko, Soft Matter **8**, 11018 (2012).
[9]Y. Xue, H. Wang, Y. Zhao, L. Dai, L. Feng, X. Wang, and T. Lin, Adv. Mater. **22**, 4814 (2010).
[10]Y. Zhao, J. Fang, H. Wang, X. Wang, and T. Lin, Adv. Mater. **22**, 707 (2010).
[11]J. Tian, T. Arbatan, X. Li, and W. Shen, Chem. Commun. **46**, 4734 (2010).
[12]T. Arbatan, L. Li, J. Tian, and W. Shen, Adv. Healthcare Mater. **1**, 80 (2012).
[13]F. Sarvi, K. Jain, T. Arbatan, P. J. Verma, K. Hourigan, M. C. Thompson, W. Shen, and P. P. Y. Chan, Adv. Healthcare Mater. **4**, 77 (2015).
[14]H. K. Lee, Y. H. Lee, I. Y. Phang, J. Wei, Y. E. Miao, T. Liu, and X. Y. Ling, Angew. Chem.-Int. Ed. **53**, 5054 (2014).
[15]W. Gao, H. K. Lee, J. Hobley, T. Liu, I. Y. Phang, and X. Y. Ling, Angew. Chem. -Int. Ed. **54**, 3993 (2015).
[16]L. Frenz, A. El Harrak, M. Pauly, S. Bégin-Colin, A. D. Griffiths, and J. Baret, Angew. Chem. Int. Ed. **47**, 6817 (2008).
[17]Y. Sheng, G. Sun, J. Wu, G. Ma, and T. Ngai, Angew. Chem. **127**, 7118 (2015).
[18]Z. Liu, Y. Zhang, C. Chen, T. Yang, J. Wang, L. Guo, P. Liu, and T. Kong, Small **15**, 1804549 (2019).
[19]Z. Liu, X. Fu, B. P. Binks, and H. C. Shum, Langmuir **31**, 11236 (2015).
[20]X. Li, R. Wang, H. Shi, and B. Song, Appl. Phys. Lett. **113**, 101602 (2018).
[21]X. Li, Y. Xue, P. Lv, H. Lin, F. Du, Y. Hu, J. Shen, and H. Duan, Soft Matter **12**, 1655 (2016).
[22]A. Rendos, N. Alsharif, B. L. Kim, and K. A. Brown, Soft Matter **13**, 8903 (2017).
[23]H.-N. Polwaththe-Gallage, C. H. Ooi, J. Jin, E. Sauret, N.-T. Nguyen, Z. Li, and Y. Gu, Appl. Phys. Lett. **114**, 43701 (2019).
[24]S. Asare-Asher, J. N. Connor, and R. Sedev, J. Colloid Interface Sci. **449**, 341 (2015).
[25]G. Whyman and E. Bormashenko, J. Colloid Interface Sci. **457**, 148 (2015).
[26]E. Bormashenko, R. Pogreb, G. Whyman, and A. Musin, Colloids Surf. A **351**, 78 (2009).
[27]X. Li, Y. Wang, J. Huang, Y. Yang, R. Wang, X. Geng, and D. Zang, Appl. Phys. Lett. **111**, 261604 (2017).
[28]X. Li, R. Wang, S. Huang, Y. Wang, and H. Shi, Soft Matter **14**, 9877 (2018).
[29]P. S. Bhosale, M. V. Panchagnula, and H. A. Stretz, Appl. Phys. Lett. **93**, 34109 (2008).
[30]J. O. Marston, S. T. Thoroddsen, W. K. Ng, and R. B. H. Tan, Powder Technol. **203**, 223 (2010).
[31]D. Zang, Z. Chen, Y. Zhang, K. Lin, X. Geng, and B. P. Binks, Soft Matter **9**, 5067 (2013).
[32]D. G. A. L. Aarts, H. N. W. Lekkerkerker, H. Guo, G. H. Wegdam, and D. Bonn, Phys. Rev. Lett. **95**, 164503 (2005).
[33]E. Bormashenko, A. Musin, G. Whyman, Z. Barkay, A. Starostin, V. Valtsifer, and V. Strelnikov, Colloids Surf. A **425**, 15 (2013).